Broadband coherent light generation in a Raman-active crystal driven by two-color femtosecond laser pulses

Miaochan Zhi* and Alexei V. Sokolov

Department of Physics and Institute for Quantum Studies, Texas A&M University, College Station, Texas 77840-4242, USA

**Corresponding author: mczhi@neo.tamu.edu*

Received April 17, 2007; accepted May 18, 2007;
posted June 28, 2007 (Doc. ID 82142); published July 26, 2007

We demonstrate broadband light generation by focusing two-color ultrashort laser pulses into a Raman-active crystal, lead tungstate ($PbWO_4$). As many as 20 anti-Stokes and 2 Stokes fields are generated due to strong near-resonant excitation of a Raman transition. The generated spectrum extends from the infrared, through the visible region, to the ultraviolet, and it consists of discrete spatially separated sidebands. Our measurements confirm good mutual spatial and temporal coherence among the generated fields and open possibilities for synthesis of subfemtosecond light waveforms. © 2007 Optical Society of America

OCIS codes: 190.5650, 190.5890, 190.4720, 320.2250.

Recently, broadband collinear Raman generation in molecular gases has been used to produce mutually coherent equidistant frequency sidebands spanning several octaves of optical bandwidths [1]. It has been argued that these sidebands can be used to synthesize optical pulses as short as a fraction of a femtosecond (fs) [2]. The technique relied on adiabatic preparation of near-maximal molecular coherence. While at present isolated attosecond x-ray pulses are obtained by high-harmonic generation [3], the Raman technique shows promise for highly efficient production of such ultrashort pulses in the near-visible spectral region, where such pulses inevitably express a single-cycle nature and may allow nonsinusoidal field synthesis [2].

We report a comparably broadband sideband generation in a Raman-active crystal (of a type that can also be used in a Raman laser [4]). We apply two 50 fs laser pulses tuned close to the Raman resonance and obtain generation of sidebands covering the infrared, visible, and ultraviolet spectral regions. The experiments with molecular gases often used nanosecond (ns) driving laser pulses, with pulse duration somewhat shorter than the Raman coherence lifetime (even though successful experiments were also performed by using fs pulses [5,6]). Since coherence lifetime in a solid is typically shorter than in a gas, the use of fs (or possibly picosecond (ps)) pulses is inevitable when working with room-temperature crystals. For example, coherent high-order anti-Stokes (AS) scattering has been observed in $YFeO_3$ and $KTaO_3$ crystals when two-color fs pulses were used [7–9], and impulsive Raman scattering was observed in $KGd(WO_4)_2$ [10].

In our experiments we use two computer-controlled optical parametric amplifiers (OPerA, Coherent), pumped by an amplified fs laser (Mira + Legend, Coherent). We obtain up to 30 μJ per 50 fs pulse at 1 kHz repetition rate (with 4% energy fluctuations) at tunable visible wavelengths. The pulses are near transform-limited, with a smooth single-peaked spectrum. They are attenuated to 1 to 2 μJ per pulse and focused to about 100 μm spot size at the sample. This laser intensity is right below the onset of strong self-phase modulation.

We use lead tungstate ($PbWO_4$), which exhibits good optical transparency and a high damage threshold and is nonhygroscopic. $PbWO_4$ has a strong narrow Raman line at 901 cm^{-1} with linewidth $\Delta\nu_R = 4.3$ cm^{-1}, which corresponds to a phonon relaxation time $T_2 \approx 2.5$ ps [11]. Our sample is 1 mm thick, and the laser beams are typically sent perpendicular to its surface and parallel to the crystalline a-axis.

In the past, when much longer single-color 100 ps pulses were applied to $PbWO_4$ (steady state regime, pulse duration $\tau_p \gg T_2$), several high-order Stokes (S) and AS sidebands were generated [12]. By using two-color ultrashort pulses (transient regime, $\tau_p \ll T_2$) that cross at the crystal at an angle of 4°, we obtain efficient generation of multiple sidebands (Fig. 1). For simplicity we call them S and AS sidebands of multiple orders, even though they are not always

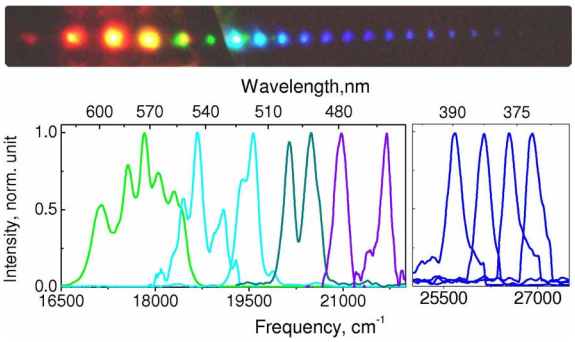

Fig. 1. (Color online) Broadband generation in a $PbWO_4$ crystal with two pulses ($\lambda_1 = 620$ nm and $\lambda_2 = 588$ nm) applied at an angle of 4° to each other. Top, generated beams projected onto a white screen. The two pump pulses (bright spots at the left), two S and two AS are attenuated by a neutral-density filter. Bottom, normalized spectra of the generated sidebands (left, AS 1 to AS6; right, AS 12 to AS 16).

0146-9592/07/152251-3/$15.00

equally spaced in frequency. We use two beams (at wavelengths $\lambda_1=620$ nm, $\lambda_2=588$ nm, and frequency separation $\delta\nu=\nu_2-\nu_1=930\ \mathrm{cm}^{-1}$) with parallel polarizations. The generated sidebands emerge spatially well separated and have the same polarization as the two input beams. Up to 20 AS and 2 S sidebands are observed on a white screen (Fig. 1, top). The pulse length for each individual sideband is expected to be of the order of the input pulse duration (50 fs). The spectra of the first 6 AS and the higher-order sidebands (AS 12 to AS 16) are measured with an Ocean Optics fiber-coupled spectrometer as shown in Fig. 1 (bottom). The spectra of the lower-order sidebands show a rich structure due to simultaneous excitation of several Raman lines by the large spectral width of the fs laser pulses. Takahashi *et al.* have observed a similar effect in their study of $YFeO_3$ [7]. We find that the spectral shapes of these lower-order sidebands are in addition affected by the (Raman nonresonant) instantaneous four-wave mixing (FWM) process. The slight bending of the plane in which the generated beams lie (noticeable in Fig. 1, top) is possibly due to the role of phase matching in selecting the directions and frequencies of the generated fields. The frequency spacing between the sidebands decreases gradually and reaches about 450 cm^{-1} at the highest orders measured.

When we vary the angle between the two applied laser beams (while keeping the two wavelengths fixed), we observe substantial changes in both the AS frequency shifts and the conversion efficiency. AS conversion is negligible for collinear input beams. The optimum conversion in $PbWO_4$ (for $\delta\nu=930\ \mathrm{cm}^{-1}$) is achieved when the angle between the applied beams is 4°. When the angle is further increased, AS conversion decreases, while the frequency separation of the AS sidebands goes up. Apparently, phase matching plays a critical role in the generation of multiple spectral sidebands in Raman-active crystals (as compared with the collinear Raman generation in gasses [1,2]). Even though at larger beam crossing angles the conversion efficiency is expected to decrease because of the reduced beam overlap, for angles below 7° it is the phase matching, along with the spectrum of exited Raman transitions, that determines the conversion efficiency and the frequencies generated in thin crystals.

To prove the Raman-resonant nature of sideband generation, and to separate the effect of instantaneous FWM, we tune the difference between the two applied laser frequencies ($\delta\nu$) and measure the generated AS frequencies. Figure 2 shows these generated frequencies as a function of the angle at which sidebands emerge from the $PbWO_4$ crystal. We perform this measurement at a relatively large input beam crossing angle of 6°. At this angle, and at sufficiently large $\delta\nu$ (1804 or 2002 cm^{-1}), the generated AS 1 beam splits into two slightly separated distinctively colored beams: one corresponding to (nonresonant) FWM and the other (which is much brighter) corresponding to Raman-resonant AS generation. By moving the fiber tip of the spectrometer to the location shown in Fig. 2 (inset) by an arrow, we measure the FWM frequency (as opposed to the Raman-shifted frequency measured at the center of the main AS 1 beam). We observe that as we vary $\delta\nu$ from 844 to 2002 cm^{-1} the Raman sidebands are generated at approximately the same angle and with roughly the same frequency shift from the previous order, while the FWM frequency varies as $\nu_{FWM}=2\nu_2-\nu_1$.

Next we investigate the mutual coherence among the generated sidebands. We first generate multiple AS sidebands by focusing red ($\lambda_R=718$ nm) and IR ($\lambda_{IR}=812$ nm) beams into the $PbWO_4$ crystal. Then a third (yellow) beam is sent along the direction of the generated AS 3 sideband with a matching wavelength ($\lambda_Y=574$ nm). Once overlap in frequency, space, and time is achieved, the sidebands (AS 2 to AS 7) start to visibly flicker, due to interference between signals generated through different channels. We measure the pulse energy of AS 5 on a shot-by-shot basis by using a fast photodiode.

The statistics of the AS 5 pulse energy is shown in Fig. 3. The solid black bars give the histogram (number of pulses versus AS 5 energy) with only red and IR pulses applied at the input. This histogram shows a typical normal distribution, with about 10% average variations. However, with the addition of the yellow beam at the input, the histogram of the AS 5 pulse energy (913 pulses total) transforms into a very different distribution (Fig. 3, white bars). We perform a simple calculation, that supports our qualitative understanding of this result. We consider interference of two fields (of the same frequency), whose intensities (I_1 and I_2) fluctuate within 10% of their mean values. We further assume that the relative phase of these two fields varies randomly between 0 and 2π (every value of $\triangle\phi$ being equally probable). The resultant intensity, $I=I_1+I_2+2\sqrt{I_1I_2}[\cos(\triangle\phi)]$, is expected to produce a histogram that is inversely proportional to the derivative of I with respect to $\triangle\phi$ and therefore has two peaks (at $I_1+I_2+2\sqrt{I_1I_2}$ and $I_1+I_2-2\sqrt{I_1I_2}$, where $\triangle\phi$ equals 0 and π, respec-

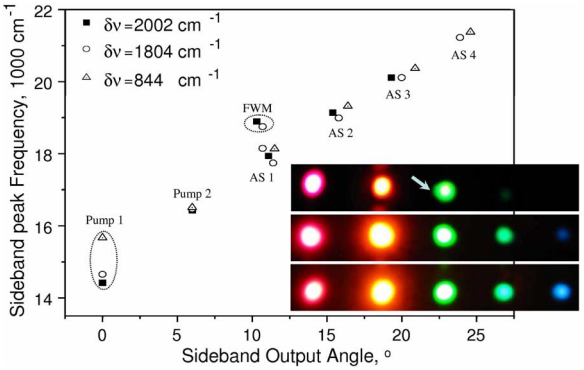

Fig. 2. (Color online) Peak frequency of the generated sidebands plotted as a function of the output angle. One input frequency (pump 2) is fixed, while the $\delta\nu=\nu_2-\nu_1$ is tuned to 844 (triangles), 1804 (circles), and 2002 cm^{-1} (squares), respectively. The FWM frequency (measured at the point shown in the inset by the arrow) varies as $\nu_{FWM}=2\nu_2-\nu_1$, while the Raman sideband frequencies stay approximately fixed. The inset shows the output beams projected onto a screen for these same values of $\delta\nu$ (varying from 2002 to 844 cm^{-1} top to bottom).

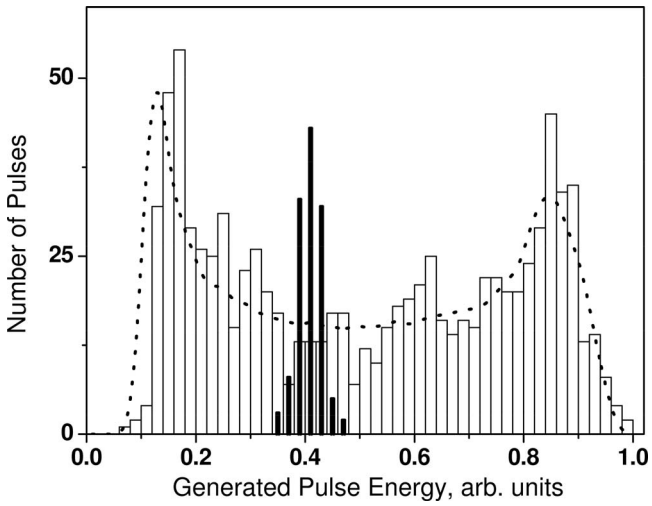

Fig. 3. Histograms of AS 5 pulse energy. Solid black bars: the number of pulses (out of 150) versus AS 5 pulse energy generated with red and IR input beams only. White bars: the histogram of AS 5 pulse energy (913 pulses total) with the addition of the third input beam. The dotted curve is a theoretical prediction obtained assuming perfect single-shot coherence of the two interfering fields and random shot-to-shot variation of their relative phase.

tively). This is exactly what our simulation shows (Fig. 3, dotted curve). In this simulation, we take the average value of $\langle I_1 \rangle = 0.41$ (arbitrary units) from the measurement and find (from the best fit in Fig. 3) $\langle I_2 \rangle = 0.09$. We repeat the calculation 91,300 times (using random number generators) and divide the calculated number of counts (per intensity) by a factor of 100 when we compare the simulation with the experiment. The two peaks in the simulated histogram appear to be broadened by the fluctuations of I_1 and I_2, which are taken to be 10% each (matching the experimental observations). The peak on the right (at higher pulse energy) is calculated to be lower and broader than the peak on the left, in excellent qualitative agreement with the experimental data. This measurement, and its comparison with theory, confirms our expectation that the (highly coherent) Raman process results in generation of mutually coherent sidebands. We expect that if the phases of the input fields are stabilized the spectral phases at the output will also be stable.

In conclusion, we have observed efficient generation of what is to our knowledge a record-large number of spectral sidebands in a Raman-active crystal driven by two-color fs pulses. The measured overall energy conversion efficiency in $PbWO_4$ is as high as 31%. We find that phase matching plays a major role in the generation process and that the instantaneous FWM signal coexist with Raman generation in the lower-order sidebands. The good mutual coherence among the spectral sidebands opens a possibility for this broadband light source to be used to synthesize subfemtosecond light waveforms.

We thank Dmitry Pestov, Xi Wang, Robert K. Murawski, Yuri Rostovtsev, Phil Hemmer, and Pengwang Zhai for helpful discussions and technical assistance. This project is supported by the Defense Advanced Research Projects Agency, the National Science Foundation (Grant no. PHY-0354897), an Award from Research Corporation, and the Robert A. Welch Foundation (Grant no. A1547).

References

1. A. V. Sokolov and S. E. Harris, J. Opt. B: Quantum Semiclassical Opt. **5**, R1 (2003).
2. A. V. Sokolov, M. Y. Shverdin, D. R. Walker, D. D. Yavuz, A. M. Burzo, G. Y. Yin, and S. E. Harris, J. Mod. Opt. **52**, 285 (2005).
3. R. Kienberger, E. Goulielmakis, M. Uiberacker, A. Baltuska, V. Yakovlev, F. Bammer, A. Scrinzi, T. Westerwalbesloh, U. Kleineberg, U. Heinzmann, M. Drescher, and F. Krausz, Nature **427**, 817 (2004).
4. H. M. Pask, Prog. Quantum Electron. **27**, 3 (2003).
5. A. Nazarkin, G. Korn, M. Wittmann, and T. Elsaesser, Phys. Rev. Lett. **83**, 2560 (1999).
6. E. Sali, K. J. Mendham, J. W. G. Tisch, T. Halfmann, and J. P. Marangos, Opt. Lett. **29**, 495 (2005).
7. J. Takahashi, Y. Kawabe, and E. Hanamura, Opt. Express **12**, 1185 (2004).
8. E. Matsubabra, K. Inoue, and E. Hanamura, J. Phys. Soc. Jpn. **75**, 024712 (2006).
9. H. Matsuki, K. Inoue, and E. Hanamura, Phys. Rev. B **75**, 024102 (2007).
10. A. S. Grabtchikov, R. V. Chulkov, V. A. Orlovich, M. Schmitt, R. Maksimenko, and W. Kiefer, Opt. Lett. **28**, 926 (2003).
11. A. A. Kaminskii, H. J. Eichler, K.-i. Ueda, N. V. Klassen, B. S. Redkin, L. E. Li, J. Findeisen, D. Jaque, J. Garca-Sole, J. Fernandez, and R. Balda, Appl. Opt. **38**, 4533 (1999).
12. A. A. Kaminskii, C. L. McCray, H. R. Lee, S. W. Lee, D. A. Temple, T. H. Chyba, W. D. Marsh, J. C. Barnes, A. N. Annanenkov, V. D. Legun, H. J. Eichler, G. M. A. Gad, and K. Ueda, Opt. Commun. **183**, 277 (2000).